Elastic Multiparameter Full-Waveform Inversion: basic theory, practice, and examples - a tutorial

Fabio Mancini[1], Tom Rayment[1] and James McLeman[1]

ABSTRACT

Full-waveform inversion (FWI) is a wave-equation-based technique that updates subsurface models until synthetic seismograms match recorded data. Originally developed for velocity model building in the acoustic approximation, FWI has evolved into a robust elastic, multiparameter framework capable of estimating P-wave velocity (V_P), density, and S-wave velocity (V_S), delivering amplitude-versus-angle (AVA) consistent rock property volumes. This tutorial outlines the theoretical basis of FWI, discusses frequency stepping, sensitivity kernels, and objective functions, and explains how elastic MP-FWI overcomes parameter trade-offs and cycle-skipping. Quality control methods and validation strategies are shown. The workflow is illustrated with a case study from the North-West Shelf of Australia, where elastic MP-FWI applied to a legacy streamer dataset produced an excellent reflectivity image and elastic parameters which matched the well ties with a high degree of accuracy.

INTRODUCTION

The increasing geological complexity in which hydrocarbons are identified has driven the development of imaging technologies to produce high-resolution amplitude-versus-angle (AVA) models to reduce exploration and production risk. Conventional workflows to derive such models have relied on imaging methods such as reverse-time migration (RTM) or Kirchhoff depth migration (KDM), both of which impose assumptions like the single-scattering Born approximation. These methods can produce pre-stack image gathers or angle stacks that are used in a secondary inversion step to determine elastic attributes like P-impedance and V_P/V_S ratio (Aki and Richards, 2002). While the least-squares imaging extensions of such techniques (Nemeth et al., 1999) enhance the amplitude fidelity and improve subsurface illumination compensation, their assumptions still ultimately limit their resolution and amplitude fidelity in regions with high impedance contrasts or complex geology.

Furthermore, conventional workflows to derive such AVA-models often involve many subjective, time-intensive data pre-processing steps to remove components of the recorded wavefield that do not agree with the assumptions imposed by the conventional imaging algorithms, such as multiples.

Full-waveform inversion (FWI) is a wave-equation-based inversion technique in which subsurface models are updated iteratively until synthetic seismograms reproduce observed field data. First introduced in its modern form by Tarantola (1984), FWI was initially constrained to recovering large-scale velocity variations from diving waves. Over the past two decades, advances in computational power and algorithms have allowed FWI to evolve into a robust technique that incorporates reflected arrivals, free surface and interbed multiples, and elastic wave phenomena (Virieux and Operto, 2009).

In its elastic, multiparameter formulation (MP-FWI), the method extends beyond P-wave velocity (V_P) to simultaneously estimate additional parameters such as S-wave velocity (V_S or in the form of V_S/V_P), density, and P and S impedances (Badry and McLeman, 2025). By jointly resolving these elastic properties, MP-FWI produces AVA-consistent models that can be validated against well logs and used directly for quantitative interpretation. This tutorial introduces the theoretical foundation of FWI, explains its extension to elastic MP-FWI, and discusses practical considerations such as frequency stepping, source wavelet requirements, and validation. Finally, an application to a legacy towed-streamer survey from offshore north-west Australia demonstrates the principles in practice.

THEORY OF FULL-WAVEFORM INVERSION

FWI seeks to minimize the misfit between observed data and synthetic data generated from an Earth model

[1]DUG Technology. | http://dx.doi.org/10.63606/ghz-0972-7132-2-2025-14
Email: fabiom@dug.com; tomr@dug.com; jamesm@dug.com

(Figure 1). The process can be understood as a three-step loop:

1. *forward modelling*: starting from an initial Earth model(s), an accurate source wavelet and the field acquisition geometry, the wave equation is solved to propagate (simulate) the wavefield in time and space, producing synthetic data (d_{syn}).
2. *compare*: these synthetic data are compared with the observed field recordings (d_{obs}). An objective function, typically the least-squares objective function given by $\frac{1}{2} \| d_{syn} - d_{obs} \|^2$, quantifies the misfit, and their difference ($d_{obs} - d_{syn}$) forms the residuals.
3. *gradient update:* the gradient of this misfit is computed efficiently using the adjoint-state method, which correlates the forward-propagated source wavefield with the back-propagated residual wavefield to update all model parameters simultaneously (Plessix, 2006). The gradient indicates the direction in which the model(s) used to simulate d_{syn} need to change to minimise the objective function.

This loop is repeated iteratively, reducing the mismatch between observed and synthetic data at each cycle. Over successive iterations, the Earth model(s) converges toward one that explains the full wavefield more accurately, ultimately producing a clearer and more reliable representation of subsurface structures.

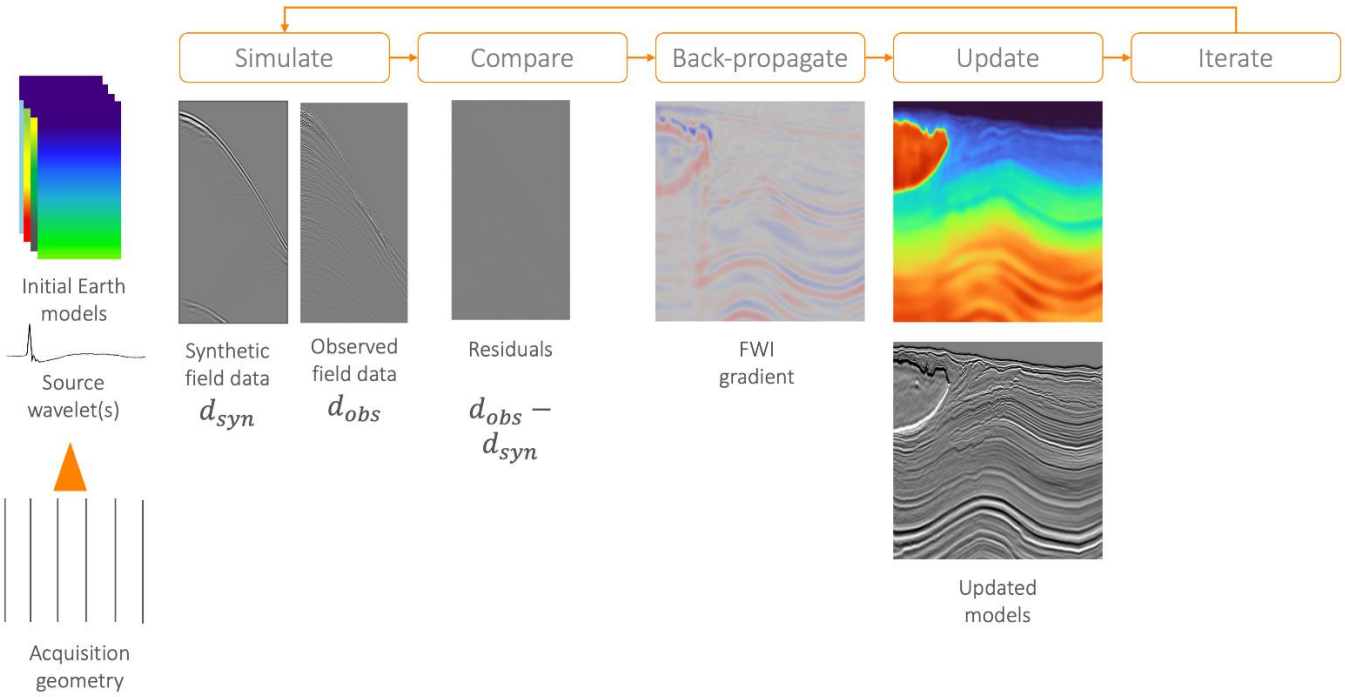


***Figure 1**: Basic FWI workflow. See text for details.*

In the forward modelling, different implementations of the wave equation can be used that have varying levels of approximation:

- *acoustic*, where the modelling is restricted to P-waves.
- *visco-acoustic*, where the modelling includes absorption effects (the quality factor, Q) for P-waves.
- *elastic (and visco-elastic)*, where the modelling includes both P- and S-waves (including absorption effects in the visco-elastic case), as well as surface waves (Figure 2).

For each of the previous cases, different levels of seismic anisotropy are considered, ranging from the simplest isotropic case, where seismic velocities are identical in all directions, to progressively more complex models. These include VTI (Vertical Transverse Isotropy), which

© SPG India. All rights reserved.

represents horizontal layering with a vertical axis of symmetry; TTI (Tilted Transverse Isotropy), where the symmetry axis is inclined to capture dipping or folded strata; and tilted orthorhombic anisotropy, which allows three orthogonal but tilted symmetry planes to account for both layering and multiple fracture sets (Thomsen, 1986).

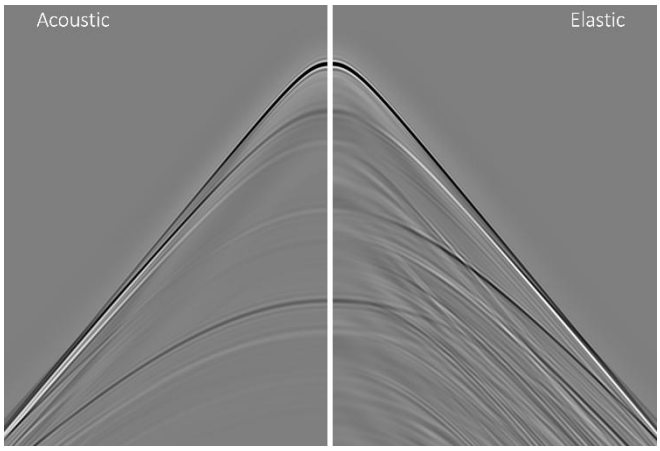


***Figure 2**: Synthetic shot gather simulated over the same earth model. Left, an acoustic wave equation is used to model the data and, right, the data are modelled with an elastic wave equation. Notice the strong effect of shear waves in the elastic simulation.*

PRACTICAL APPROACHES

In practice, FWI workflows will not try to fit the entire seismic wavefield from the beginning. FWI strategies will focus on matching part of the wavefield and then gradually include more information (Warner et al., 2013). Generally, FWI will start by matching the low frequencies only, gradually including higher and higher frequencies, in order to mitigate the risk of cycle-skipping. Cycle-skipping occurs when the phase difference between observed data and synthetic data exceeds half a cycle, and the inversion converges to an incorrect minimum, also called a local minimum.

Frequently, FWI will also initially focus on the direct transmitted wavefield (diving waves), before incorporating information from the reflected wavefield. It might initially focus on the phase of the wavefield (mostly sensitive to velocity changes), before the amplitudes are incorporated, as they are influenced not just by velocity but also by density variations and the V_P/V_S ratio. The sensitivity of amplitudes can be fully leveraged when FWI incorporates the correct wave physics, enabling the inversion to recover not only velocity but also density and V_P/V_S parameters directly from seismic data. By doing so, FWI provides a pathway to characterize both lithology and fluid content, offering a more complete description of subsurface properties.

OBJECTIVE FUNCTIONS

The classical least-squares objective is computationally efficient but sensitive to cycle-skipping. Cycle-skipping happens when the starting model is too far from the true subsurface properties and the observed data and the synthetic data are out of step by more than half a cycle. In that case, instead of aligning the two correctly, the inversion mistakenly lines them up with the wrong peak or trough of the wave. This traps the solution in a false match, or local minimum, and prevents the model from moving toward the true Earth structure. To address this, several families of alternative objective functions have been developed:

- *amplitude–phase decompositions*: envelope-based misfits (Wu et al., 2014) compare instantaneous amplitudes rather than raw waveforms, making them less sensitive to absolute phase differences. Phase-only approaches, such as travel time-based inversion (Luo & Schuster, 1991) or explicit phase-objective functions (Ma and Hale, 2013), focus on event alignment while ignoring amplitude.
- *distance-based misfits*: cross-correlation measures offer a straightforward way to track timing alignment between observed and synthetic data. Examples include template-matching (Cheng et al., 2023) and dynamic-matching (Mao et al., 2020). Another approach is the multi-dimensional optimal transport formulation (Métivier et al., 2016), which treats seismic traces as probability distributions and quantifies the cost of morphing one distribution into another. By aligning events globally, the Wasserstein distance produces less oscillatory and more convex-like objective functions, reducing the risk of cycle-skipping.
- *filter-based misfits*: Adaptive Waveform Inversion (AWI; Warner and Guasch, 2016) represents an example of this class. Instead of minimizing the waveform difference directly, AWI estimates an adaptive matching filter that maps modelled data to observed data. The inversion then penalizes deviations of this filter

© SPG India. All rights reserved.

from an ideal delta function. This reframing of the misfit into a filter-estimation problem broadens the basin of attraction and improves robustness in the absence of very low frequencies.

In practice, often these formulations like AWI or optimal transport are used in the early stages to mitigate cycle-skipping and establish the low-wavenumber background model. The inversion then transitions to the least-squares objective function to recover amplitudes and fine-scale detail at higher frequencies.

MULTIPARAMETER FWI

In multiparameter FWI (MP-FWI), both the kinematic and dynamic information contained in the scattered wavefield are exploited simultaneously. A core feature of the method is the ability to decouple the "rabbit ears" (the kinematic term) from the migration smile (the dynamic term) in the reflected wavefield (see Figure 3). This separation is significant because the kinematic component primarily drives velocity updates, while the dynamic component carries the amplitude variations that define reflectivity. Reflectivity, in turn, is directly linked to impedance contrasts, which depend on velocity, density, and V_P/V_S ratio. By isolating the two contributions, MP-FWI not only recovers an accurate velocity model but also derives a true-amplitude reflectivity image, without crosstalk between the two effects.

The practical implications are substantial. First, using the kinematic portion of the reflections makes it possible to update velocity at depths that extend well beyond the penetration of diving waves. Traditional FWI is inherently limited by the maximum offset of diving energy, which constrains model updates to the shallow subsurface. Reflection-based updates in MP-FWI overcome this limit, extending velocity building to the maximum depth of the recorded data.

Second, by retaining the full dynamic content of the wavefield, MP-FWI supports least-squares imaging of primaries, ghosts, surface-related multiples, and interbed multiples alike. This differs fundamentally from conventional imaging approaches, which rely exclusively on primaries. Incorporating all orders of multiples not only improves illumination but also enhances amplitude fidelity, producing reflectivity models that are more consistent with the true Earth response.

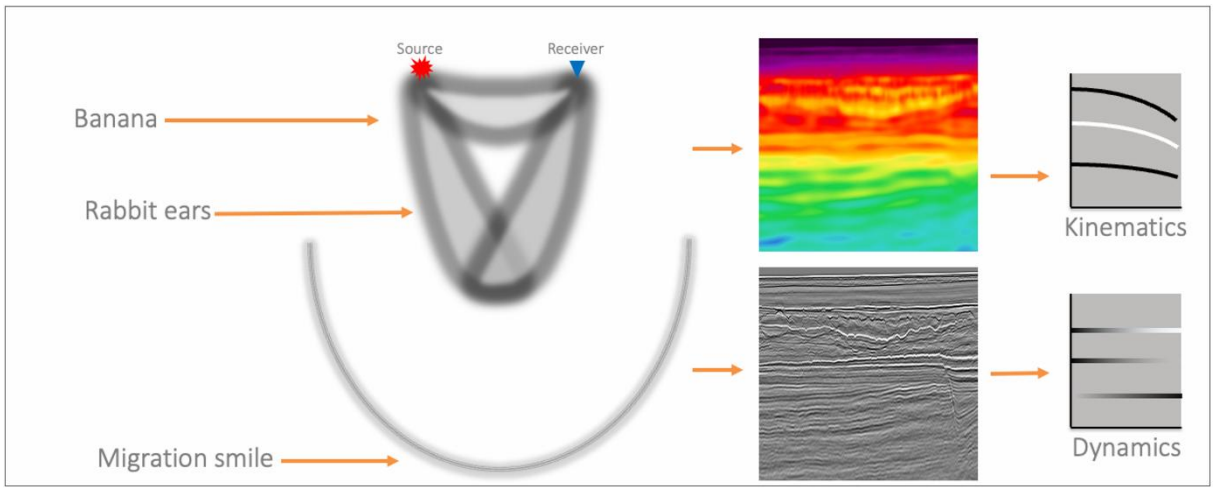


***Figure 3**: Separating the kinematic (rabbit ears) and dynamic parts (migration smile) of the scattered wavefield to produce pure kinematic and pure dynamic attributes. The banana term is from the diving waves and carries kinematic information.*

SOURCE WAVELET CONSIDERATIONS IN FWI

The source wavelet is a critical input for full-waveform inversion, particularly when simultaneously solving for primaries and multiples to achieve true-amplitude reflectivity. A properly defined wavelet ensures that both the phase and the amplitude of the modelled data are consistent with the field data. Key requirements are

- *Ghost-free*: free-surface effects are modelled explicitly within the FWI wavefield propagation.

© SPG India. All rights reserved.

- *Consistent filtering*: hydrophone response, acquisition filters, and any additional processing filters must be applied identically to the source wavelet and the recorded seismic data.
- *Amplitude fidelity*: unlike diving-wave FWI where bulk amplitude normalization is often acceptable, in MP-FWI accurate absolute amplitude is essential to resolve both primaries and multiples.

There are two main options to derive the wavelets, in preferred order:

- *near-field hydrophones (NFH).* With reliable calibration, NFH will typically provide the most suitable wavelet. Shot-to-shot far-field signatures as well as notional signatures (signatures of each gun in the array) can be derived;
- *modelled signatures*. These can be used, but often fail to represent the embedded dataset wavelet, especially at low frequencies. In this case source wavelet inversion can be performed, see Figure 4. One wavelet per shot is estimated by minimizing residuals between modelled and observed data using the direct arrival. The output can be used per shot or averaged across a survey.

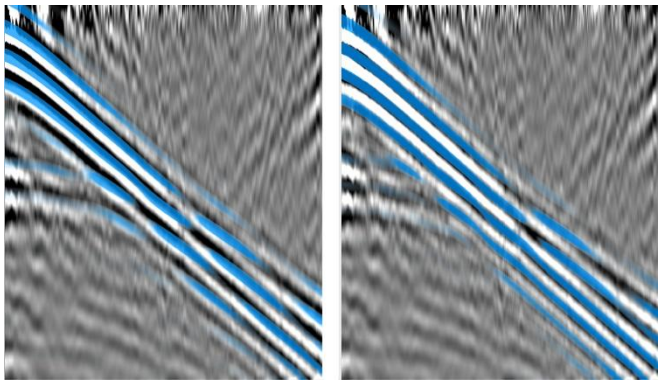


***Figure 4**: Source wavelet inversion. Synthetic data, in blue, overlaid on observed data, grayscale. The blue of the synthetics should be on top of the black peak of the observed. Left, before wavelet inversion and, right, after wavelet inversion.*

As mentioned, accurate wavelet amplitude is essential. If direct arrivals are visible, wavelet amplitudes can be calibrated against them. Comparisons between observed and modelled seafloor amplitudes guide corrections by scaling the wavelet and adjusting velocity/density contrasts until both primaries and multiples match.

QUALITY CONTROL

A reliable inversion must reproduce the kinematics and dynamics of the recorded data. Quality control therefore focuses on consistency between field and synthetic seismograms and on the reflectivity models. Fundamental QCs include:

- overlaying modelled and observed data both in the shot domain and receiver domain, at the considered frequency, with cross-correlation metrics (time shift and cross-correlation coefficient);
- performing global cross-correlation between modelled and observed data at the considered frequency and for selected offsets (Figure 5);
- overlaying the updated velocity model with the reflectivity to ensure geological consistency of the updates;
- generating FWI angle gathers to ensure residual move-out is reduced;
- validating the output parameters, V_P, density, V_P/V_S, with available well logs at the considered frequency.

DATA EXAMPLE: STREAMER ACQUISITION IN THE NORTH-WEST SHELF, AUSTRALIA

This dataset was acquired in 2006 using a dual-source towed-streamer array northwest of Barrow Island. The towed-streamer vessel consisted of eight streamers with 6 km maximum offsets. The geology in the survey area is characterized by shallow carbonate heterogeneities and complex channel features.

Legacy V_P models were initially refined using diving-wave FWI up to 19 Hz. Initial low-frequency models for V_S/V_P and density were built using well logs and regional geological knowledge. These inputs were used in a multi-stage visco-elastic MP-FWI workflow: V_P and P-impedance were first updated at 11 Hz, 14 Hz, and 19 Hz; anisotropy was refined at 19 Hz; and a targeted single-parameter inversion further improved P-impedance using near-angle reflections. The inversion for V_P, V_S/V_P, and P-impedance followed at 19 Hz, 25 Hz, 35 Hz and 60 Hz.

© SPG India. All rights reserved.

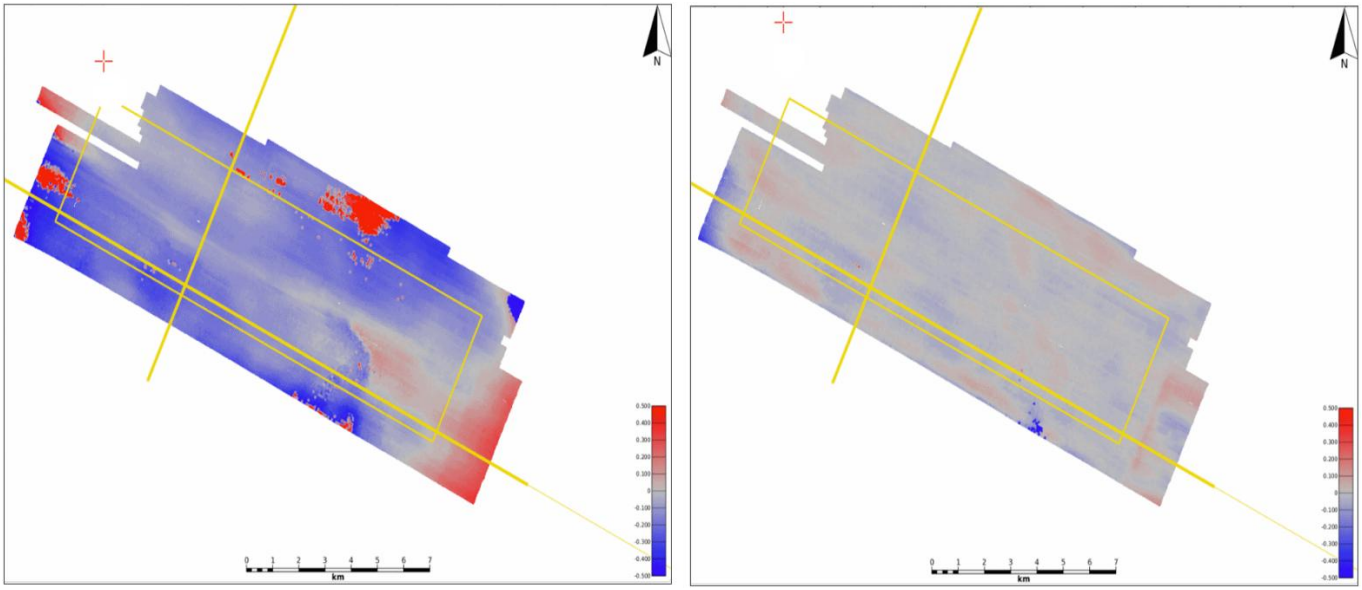


***Figure 5**: Example of global cross-correlation between modelled and observed data, expressed as the time-shift measured by cross-correlation. Left: before MP-FWI, where larger shifts indicate misalignment between synthetic and observed events. Right: after MP-FWI, where the time-shifts are reduced and closer to zero, reflecting improved event alignment.*

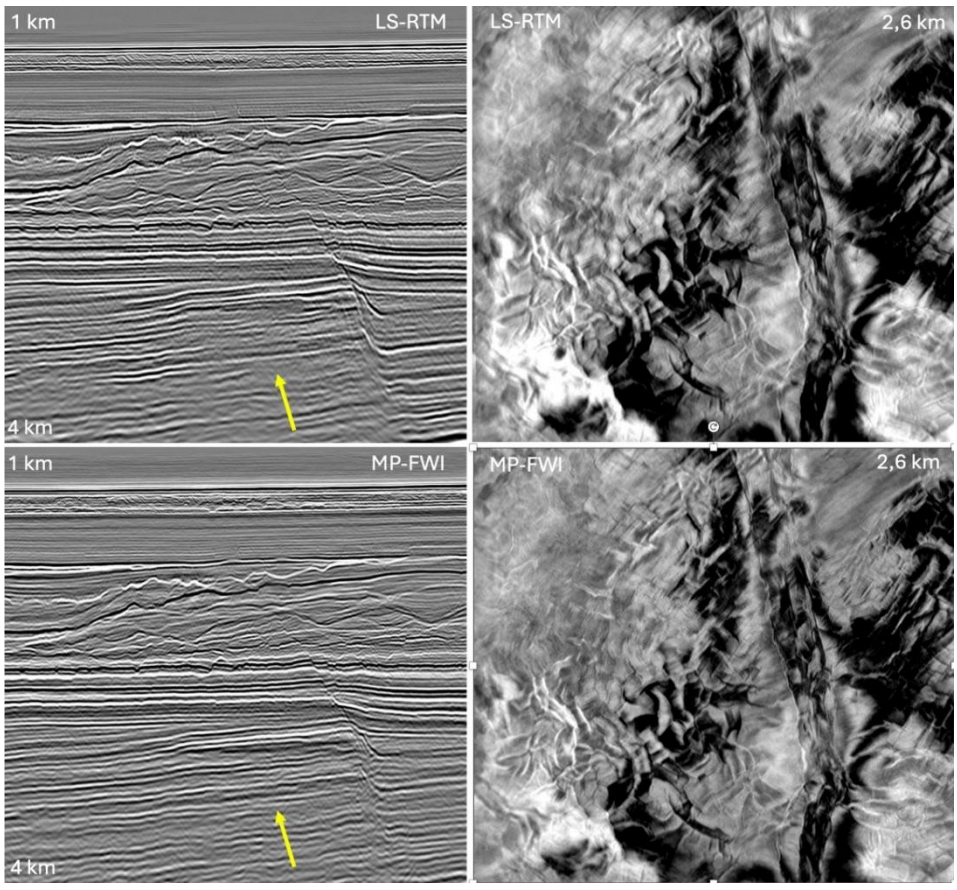


***Figure 6**: Imaging results at 60 Hz for LS-RTM (top row) and elastic MP-FWI (bottom row). Inline on the left and depth slice at 2600 m on the right.*

© SPG India. All rights reserved.

The inversion used raw hydrophone field recordings, with wavelets modelled and iteratively updated during inversion. Pre-processing was deliberately limited to preserve the full recorded wavefield; no deghosting, demultiple, or bandwidth shaping was performed.

Figure 6 compares the imaging results from least-squares RTM (LS-RTM) and visco-elastic MP-FWI at 60 Hz. Although LS-RTM used the velocity model derived from MP-FWI, its input data had undergone a full sequence of pre-migration processing. In contrast, visco-elastic MP-FWI operated directly on raw shot records. Even so, the MP-FWI reflectivity volume exhibits sharper channel definition and more coherent deep reflectors, as indicated by the yellow arrow.

The full value of visco-elastic MP-FWI is further illustrated in Figure 7, where inlines of the starting and final models for V_P, V_S/V_P ratio and density and in Figure 8 showing the starting and final models for P-impedance and S-impedance. The final results show substantial resolution gains across all parameters. Fine-scale stratigraphic features, sharp fault boundaries, and subtle lithological variations, absent in the starting models, become clearly visible in the final models. Gas bodies and their associated flat spots are well defined in the updated V_P and P-impedance volumes (see yellow arrows), while, as expected, the gas-related anomaly is weak in the inverted S-impedance, confirming the fluid sensitivity of these parameters. These improvements are entirely seismic driven as no well information was provided to the inversion itself. Wells were used only to construct the initial low-frequency background models, meaning all higher-frequency detail, stratigraphic clarity, and parameter contrasts in the final results are products of the recorded seismic wavefield. This demonstrates the method's ability to extract geologically meaningful, AVA-consistent rock property volumes directly from field data without explicit well control.

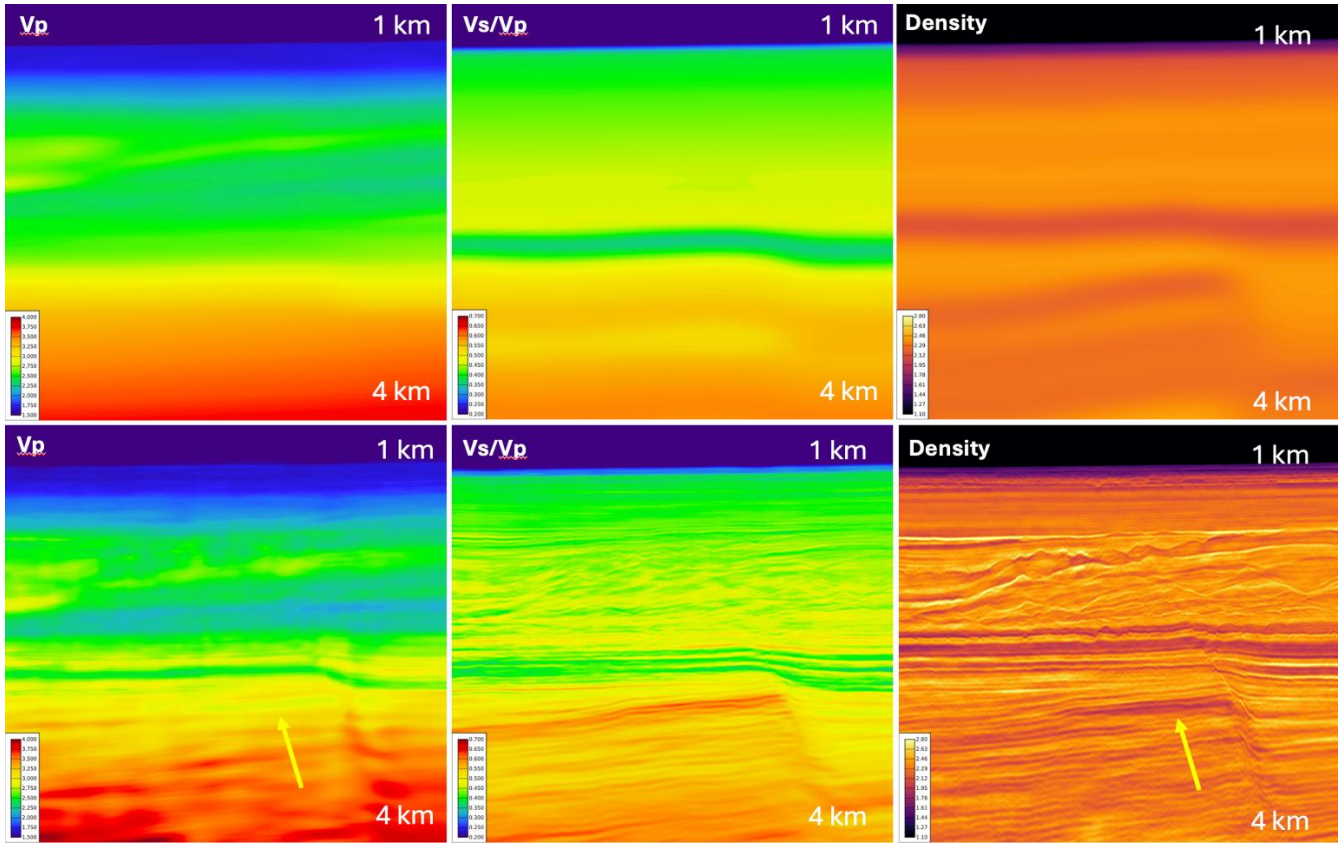


***Figure 7**: Top row: starting models of V_P, V_S/V_P and density. Bottom row: final models of V_P, V_S/V_P and density.*

© SPG India. All rights reserved.

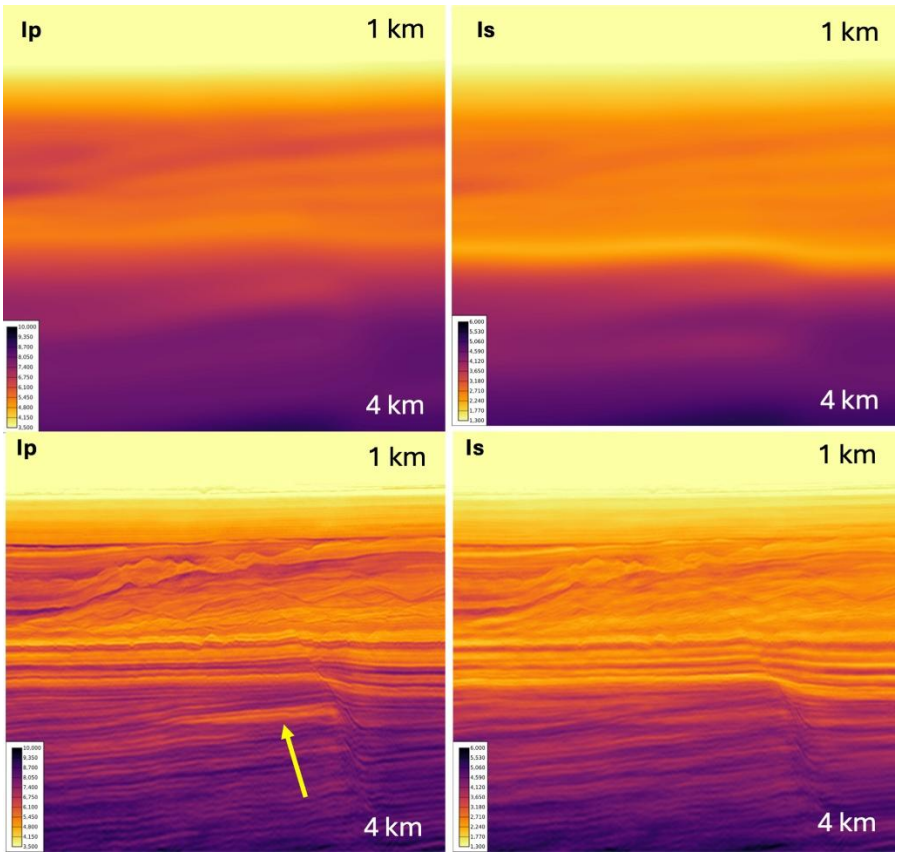


***Figure 8**: Top row: starting models of P-impedance and S-impedance. Bottom row: final models of P-impedance and S-impedance.*

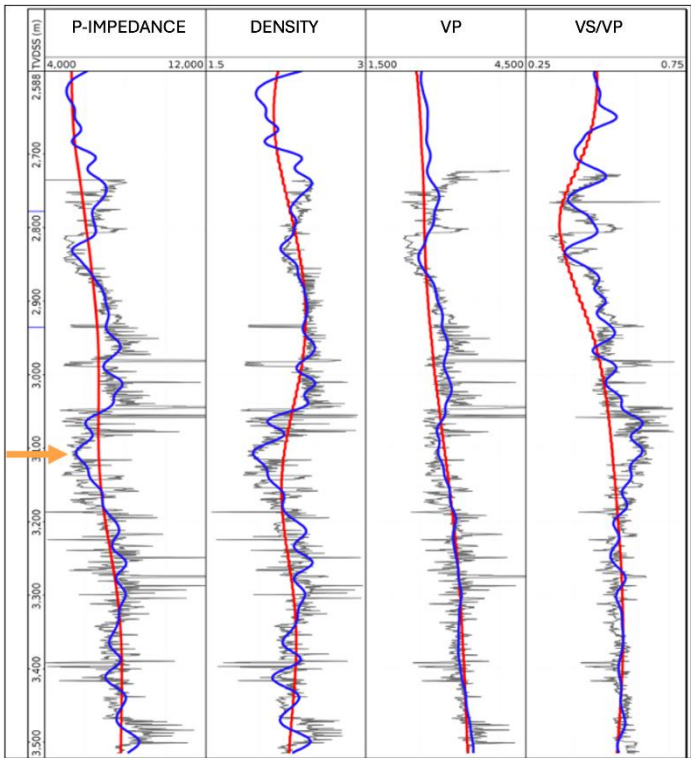


***Figure 9**: Results of P-impedance, density, V_P and V_S/V_P at the well. Well information is in grey, the initial models are in red and the visco-elastic MP-FWI models are in blue.*

© SPG India. All rights reserved.

The available wells were used to QC the results, as shown in Figure 9. Here, well information (grey), initial models (red), and final visco-elastic MP-FWI results (blue) are compared at the well location. The agreement between the inverted parameters and the measured well logs is strong across all properties, with MP-FWI accurately capturing the P-impedance drop and associated reductions in V_P and density, alongside an increase in V_S/V_P in the gas-bearing interval marked by the orange arrow. This close match provides independent validation of the inversion, confirming that the seismic-driven updates are geologically realistic, and that parameter crosstalk has been effectively mitigated.

CONCLUSIONS

Elastic multiparameter FWI extends acoustic FWI into a powerful framework for deriving AVA-consistent elastic properties. By incorporating primaries and multiples, and carefully staging frequency and parameter updates, MP-FWI produces geologically realistic models for reservoir characterization.

The North-West Shelf case study shows how legacy data can benefit substantially from this technology, with improved structural imaging compared with conventional imaging and with derivation of elastic parameters that match the well logs with a high degree of accuracy.

REFERENCES

Aki, K. and Richards, P.G., 2002, Quantitative Seismology, University Science Books, second edition.

Badry, J. and J. McLeman, 2025, Unlocking rock properties using elastic multiparameter FWI, 5th International Meeting for Applied Geoscience & Energy (IMAGE), 1-4.

Cheng, X., J. Xu, D. Vigh, and M. Hegazy, 2023, Enhanced template-matching full-waveform inversion, 85th EAGE Annual Conference and Exhibition, 1-5. https://doi.org/10.3997/2214-4609.202310765

Luo, Y., and G. T. Schuster, 1991, Wave-equation traveltime inversion, Geophysics, **56**(5), 645–653. https://doi.org/10.1190/1.1443081

Ma, Y., and D. Hale, 2013, Wave-equation reflection traveltime inversion with dynamic warping and hybrid waveform inversion, SEG Technical Program Expanded Abstracts, 871-876. https://doi.org/10.1190/segam2013-0087.1

Mao, J., J. Sheng, Y. Huang, F. Hao, and F. Liu, 2020, Multi-channel dynamic matching full-waveform inversion, SEG Technical Program Expanded Abstracts, 5056–5060. https://doi.org/10.1190/segam2020-3427610.1

Métivier, L., R. Brossier, Q. Mérigot, E. Oudet, and J. Virieux, 2016, Measuring the misfit between seismograms using an optimal transport distance, Geophys. J. Int'l, **205**, 345–377. https://doi.org/10.1093/gji/ggw014

Nemeth, T., C. Wu, and G. T. Schuster, 1999, Least-squares migration of incomplete reflection data, Geophysics, **64**(1), 208-221. https://doi.org/10.1190/1.1444517

Plessix, R.-E., 2006, A review of the adjoint-state method for computing the gradient of a functional with geophysical applications, Geophys. J. Int'l, **167**(2), 495–503. https://doi.org/10.1111/j.1365-246X.2006.02978.x

Tarantola, A., 1984, Inversion of seismic reflection data in the acoustic approximation, Geophysics, **49**(8), 1259–1266. https://doi.org/10.1190/1.1441754

Thomsen, L.,1986, Weak elastic anisotropy, Geophysics, **51**(10), 1954–1966. https://doi.org/10.1190/1.1442051

Virieux, J., and S. Operto, 2009, An overview of full waveform inversion in exploration geophysics, Geophysics, **74**(6), WCC1–WCC26. https://doi.org/10.1190/1.3238367

Warner, M., A. Ratcliffe, T. Nangoo, J. Morgan, A. Umpleby, N. Shah, V. Vinje, I. Stekl, L. Guasch, C. Win, G. Conroy, A. Bertrand, 2013, Anisotropic 3D full-waveform inversion, Geophysics, **78**(2), R59-R80. https://doi.org/10.1190/geo2012-0338.1

Warner, M., and L. Guasch, 2016, Adaptive waveform inversion: Theory, Geophysics, **81**(6), R429–R445. https://doi.org/10.1190/geo2015-0387.1

Wu, R. S., J. Luo, and B. Wu, 2014, Seismic envelope inversion and modulation signal model, Geophysics, **79**(3), WA13–WA26. https://doi.org/10.1190/geo2013-0294.1

© SPG India. All rights reserved.

BIOGRAPHIES



Fabio Mancini is a geophysicist specializing in seismic acquisition, processing, and imaging, with a strong focus on innovation. After starting at CGG in London and earning a Ph.D. in converted wave imaging from the University of Edinburgh, he worked with Total on land and marine projects before joining Hess to oversee seismic activities across the Eastern Hemisphere. At Woodside, he rose to Chief Geophysicist in 2018, driving advances in full waveform inversion and novel acquisition methods that led to the spin-off Blue Ocean Seismic Services, where he developed autonomous seismic technology. In 2025, he became Chief Geophysicist for APAC and the Americas at DUG Technology.



Tom Rayment graduated in 2004 from Imperial College with a degree in mathematics. He began his career at Fugro before joining DUG in 2013. In 2020, he was appointed Chief Geophysicist. He leads DUG's research team with an active role in the development of novel technologies, including full-waveform inversion and multiparameter full-waveform inversion imaging.



James McLeman graduated from Aberdeen University with a master's degree in physics in 2013. He then worked with CGG for five years, where he began his journey understanding seismic exploration and image processing technologies, with a special interest in extending the potential of full-waveform inversion. In 2019, James joined DUG Technology and is currently the Principal Research Geophysicist focusing on utilizing full-waveform inversion as a means to supersede many conventional processing technologies.

© SPG India. All rights reserved.